La Metallurgia Italiana
International Journal of the Italian Association for Metallurgy

Detection of Non-metallic Inclusions in 12Mn Steel Continuous Casting Round Billets

X. Wang, J. Wei, S. Qiu

Automated particle analysis was carried out to explore non-metallic inclusions in 12Mn steel continuous casting round billets, which has the features of quick obtaining the morphology, size, original positions, and composition of inclusions in a certain area. Both morphology and composition of main inclusions were calculated by using thermodynamic calculation. Meanwhile, considering the all kinds of inclusions, the spatial distribution was identified, including the distribution of oxide and sulfide inclusions. The obtained information above could be adopted to explore the source of inclusions and modify ladle refining process.

KEYWORDS: NON-METALLIC INCLUSIONS; ASPEX SCANNING ELECTRON MICROSCOPE; OPA; SLIME; 12MN STEEL; CONTINUOUS CASTING; ROUND BILLETS

INTRODUCTION

Non-metallic inclusions' characterization plays a crucial role in making clean steel. Inclusions in the final product are harmful to the quality of steel products [1, 2]. To obtain high-performance steel, the number of the inclusions have to be diminished. Generally speaking, non-metallic inclusions could be categorized as indigenous and exogenous. Indigenous inclusions stem from alloying elements which react with dissolved gas to generate solid inclusions during continuous casting. Some aspects can lead to inclusions, including deoxidation, reoxidation and solidification from reduced gas solubility. Sources outside of the liquid steel produce exogenous inclusions, such as slag entrainment or refractory wear. The evaluation methods of non-metallic inclusions are important to metallurgists, which comprise the amount, size distribution, morphology, spatial distribution, and their chemical composition. [1, 3-12]

More than twenty methods of evaluating inclusions impurities were summarized by Zhang. [1]. Metallographic microscope [13], one of these methods, is extensively used to explore size of inclusions and the two-dimensional morphology in steel. But, the chemical composition

Xu Wang, Jun Wei, Shengtao Qiu
National Engineering Research Center of Continuous Casting Technology, Central Iron and Steel Research Institute, Beijing 100081, China

of inclusions cannot be identified. Scanning electron microscopy [14] allows exploration of morphology of inclusions. Furthermore, scanning electron microscopy allows identification of the elemental composition of inclusions by exerting with energy-dispersive spectroscopy. But it is too time-intensive to count the majority of inclusions by using this method. Although acid extraction method could explore the stereoscopic morphology of inclusions, it destroys sulfide inclusions to some extent. [15–18] Involving the extraction using bromine-methanol, iron bromide dissolves rapidly, so a chelate has to be added to dissolved iron in the electrolytic approach, which is conducive to revealing the three-dimensional morphology and keeping composition of the inclusions. X-ray detection [22] and Ultrasonic inspection [19-21] are more time-saving than methods above, and could be applied for online analysis; yet the composition data and morphology are difficult to obtain. Nevertheless, other indirect methods, such as total oxygen (T.O) [23, 24] and continuous excitation of spark spectrum, have the limitations of exploring both the composition [25, 26] and the distribution of inclusions.
However, as the above mentioned papers do not address specific steel grades, in the current study typical inclusions in 12Mn steel round billets were investigated. Furthermore, the size, spatial distribution, and composition of inclusions in 12Mn steel round billets were observed.

INTRODUZIONE

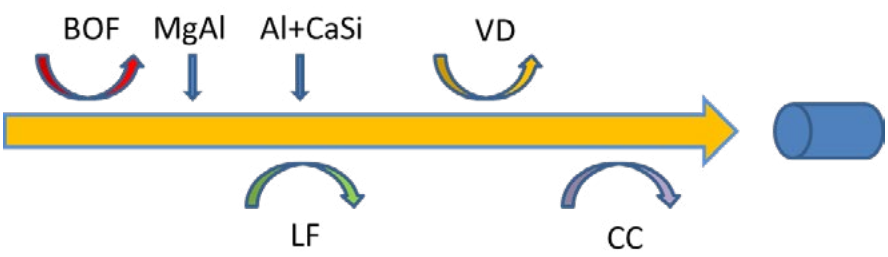

Fig.1 - Flow chart of production process of 12Mn steel round billet

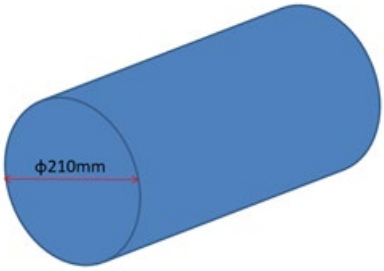

Fig.2 - Sample from 12Mn round billet

12Mn steel round billet samples were taken from continuous casting round billet which stemmed from aluminum-killed low carbon steel in a six strand CC (Fig. 1). The schematic of billet is shown in Fig. 2. The composition in 12Mn steel is illustrated in Table I. The casting speed was 1.6 m/min to 1.8 m/min leading to 40 minutes of casting time per heat. Besides, round billet samples were achieved at steady state. First, the samples were polished. Then, the 2-dimensional morphologies and compositions of inclusions in 12Mn steel samples were analyzed, assisted with using an automated SEM–EDS—ASPEX 1020 system. [27] The frame-based analysis is the automated particle analysis pattern. To begin with, the certain area was classified to some fields by the microscope. The electron beam was set on a field, then the microscope implements quick search with search steps. The intensity in back-scatter electrons was transmitted into the computer. When particle was obtained, the step size was dropped to measure the dimensions of the inclusions. The center of inclusion was illuminated, and the chord algorithm was identified to explore the particle. Last, the beam was fixed in the center of inclusions to obtain the characteristic X-ray. Through combination of steps above in corresponding field, next the beam was transformed to next field. [28, 29]

Tab.1 - Chemical composition of steel sample %

Element	C	Si	Mn	P	S	Alt	T.O
12Mn	0.1	0.28	1.24	0.013	0.002	0.03	0.0025

In the following experiment, the size distribution, rough morphology, and composition of inclusions were automatically achieved by coping with ASPEX 1020 system. Furthermore, the ASPEX has the features of quick scanning, as a result, most of the particles were tested in several hours, even though the image resolution of inclusions is not high. The sample detecting 10x15 mm^2 was measured. The beam scanned the area on the 10x15 mm^2 sample, eventually 63 mm^2 scanned area was analyzed. The minimum inclusion size was fixed at 2 μm, implying that all the inclusions size measured by the ASPEX 1020 was larger than 2 μm. The phase diagrams of inclusion is illustrated in Figure 3. Figure 4 represents the schematic of scanning area by Original Position Analysis (OPA).

After the steel samples were polished, we could obtain the two-dimensional morphologies and composition detected by using SEM-EDS. In order to obtain three-e-dimensional morphologies of non-metallic inclusions greater than 50 μm in 12Mn steel round billet, inclusions were partially extracted from samples by the method of Slime reported by Fang.[33] The scheme of the device is illustrated in Fig. 5. The electrolyte contained 89% methanol + 5% + glycerine + 5%
trithanolamine + 1% tetramethyl ammonium chloride. Argon atmosphere was implemented to prevent oxidation of 12Mn steel. The anode was cylindric with 5 mm in diameter and the cathode was 100 mm high and 60 mm in diameter. After electrolysis, non-metallic inclusions were partially extracted. At least 20 inclusions were explored with SEM-EDS.

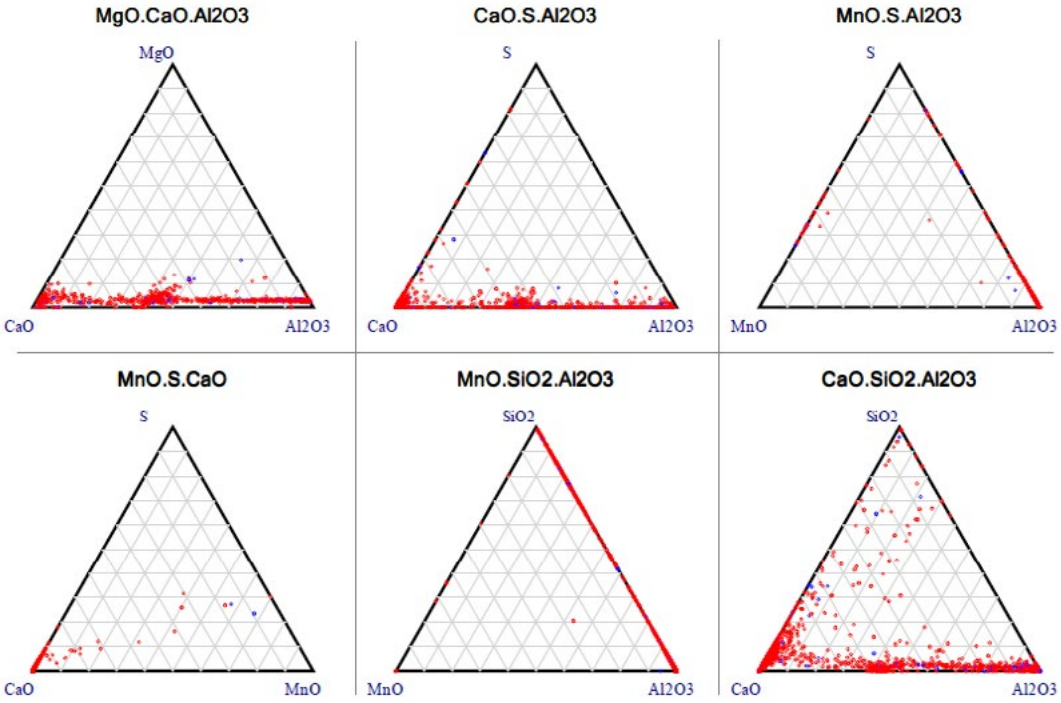

Fig.3 - Inclusion species phase diagram

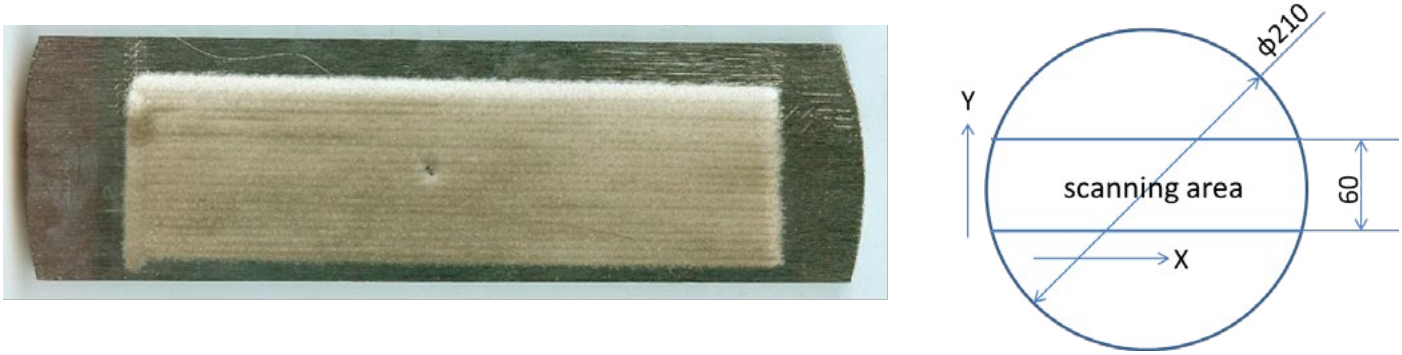

Fig.4 - Scanning area of OPA

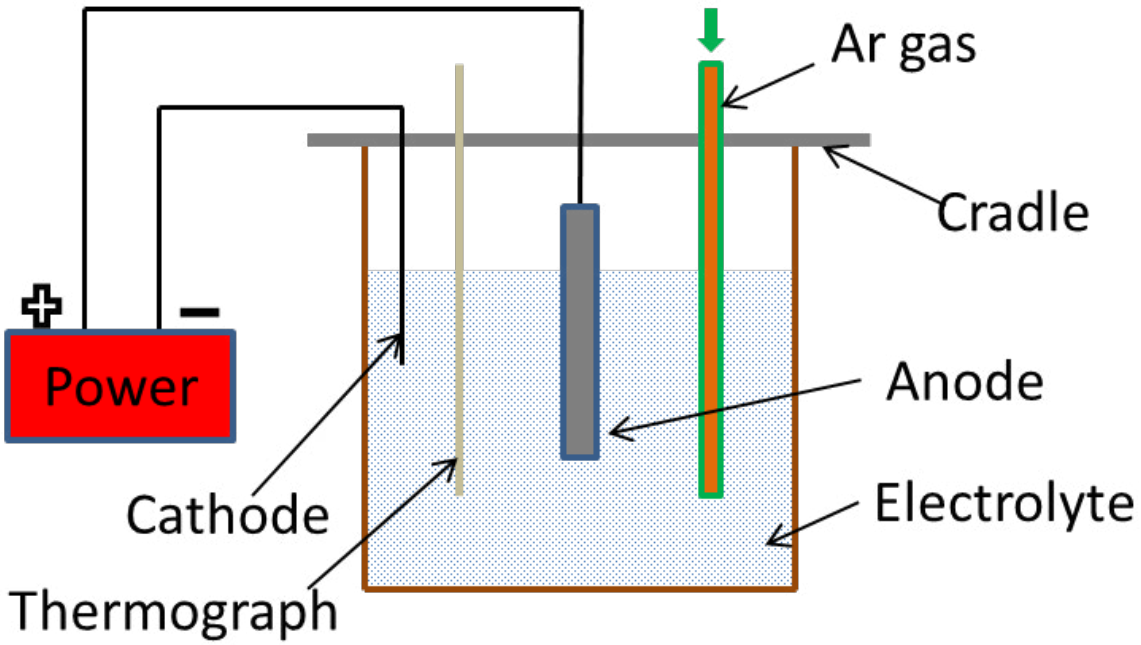

Fig 5 - Schematic of Slime to extract inclusions from 12Mn steel round billet

RESULT AND DISCUSSION

Figure 3 displays the composition of inclusions in 12Mn round billet sample using ASPEX. The typical inclusions in the 12Mn steel round billets are alumina-based clusters, cluster inclusions or alumina magnesia (Al_2O_3-MgO) spinel single, silicon oxide (SiO_2) bearing spherical inclusions, separate sulfide-based inclusions, and irregularly shaped slag inclusions containing potassium oxide (MgO), calcium oxide (CaO), and sodium oxide (Al_2O_3) shown in Figure 6. Most of alumina (Al_2O_3) inclusions originate from reoxidation. High magnesium oxide inclusions stem from the reaction between magnesium refractory and liquid steel, in particular tundish lining refractory. Sulfide inclusions precipitate on the condition of solidification of the steel. The resolution achieved by ASPEX was fixed for providing enough data to obtain the size, area, and perimeter with available detecting time and storing space for a large number of inclusions.

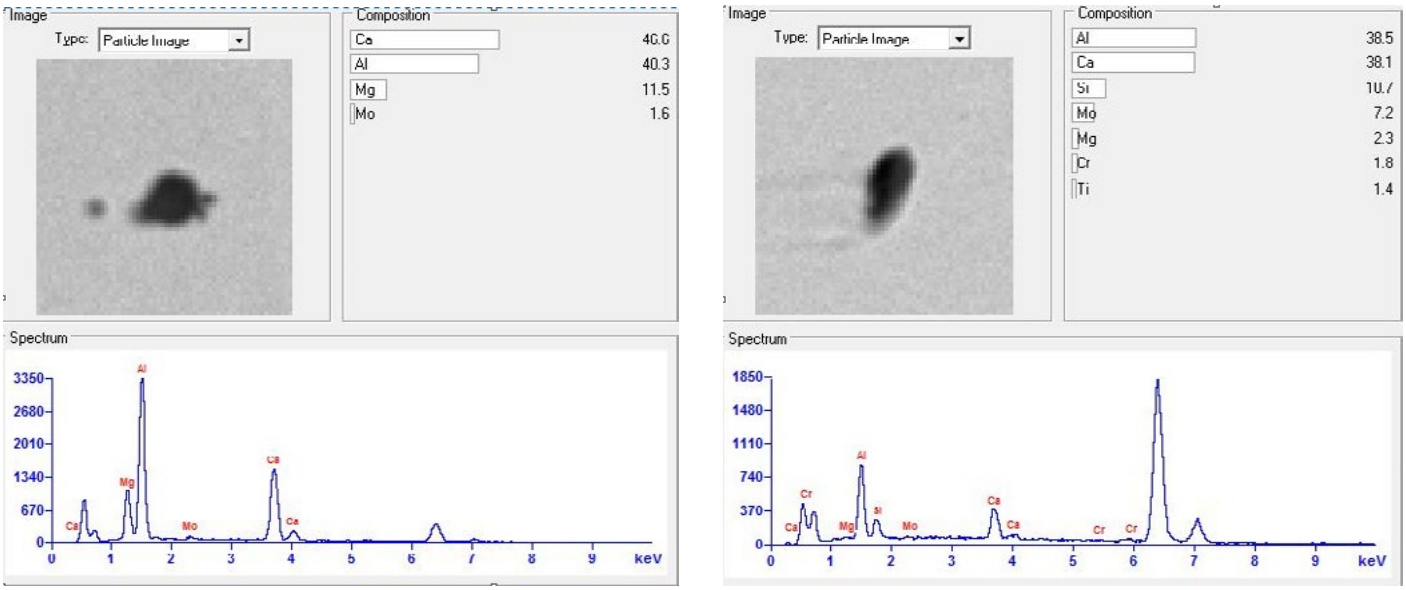

Fig.6 - Inclusion morphology and composition (mass pct) obtained by SEM.

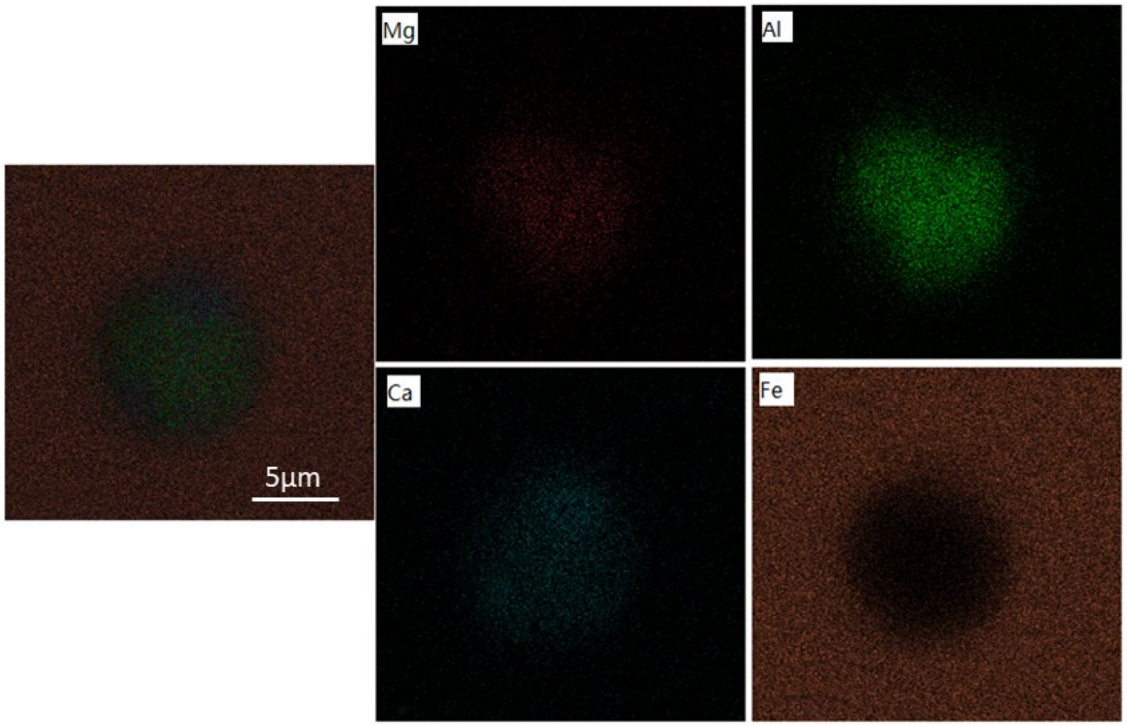

Fig.7 - Elemental mapping of typical MgO-Al_2O_3-CaO inclusions

There existed a lot of MgO-Al_2O_3-CaO complex inclusions. The morphology and composition of MgO-Al_2O_3-CaO inclusions in molten 12Mn steel are shown in Figure 7. The size of these inclusions was approximately 10 µm. The shapes of inclusions tended to be more spherical. From elemental mapping (Figure 7), the common characteristics were as follows: Al and Ca were mainly elements; little Mg content was located in the center region of MgO-Al_2O_3-CaO inclusions; and Fe content in MgO-Al_2O_3-CaO inclusions was much lower than that in other matrix regions.

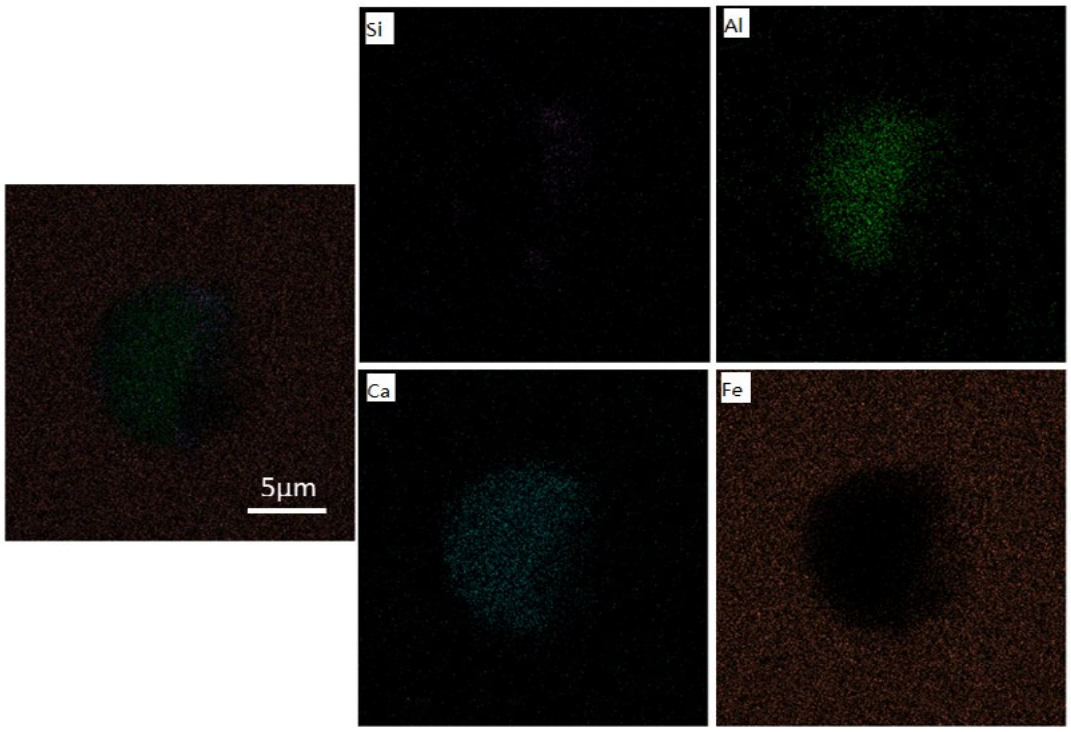

Fig.8 - Elemental mapping of typical SiO2-Al_2O_3-CaO inclusions

The elemental mappings of typical SiO_2-Al_2O_3-CaO inclusions in 12Mn steel are illustrated in Fig.8. The contents of Al and Ca are significantly higher than Si. The size of the main inclusions is about 10 μm. The area on the right shows little amounts of Silicon.

The method of OPA according to statistical analysis of more than ten thousands primary optical signals is applied in this work. The main inclusions examined by OPA are Al_2O_3-containing types and their average size is 3.3 μm calculated from Figure 9. Besides, in order to obtain the distribution of Al_2O_3-containing inclusions, we explored the line distribution (Figure 10), two-dimensional distribution (Figure 11), and three-dimensional distribution of Al (Figure 12). These results imply that Al_2O_3-containing inclusions were located in the center region of the round billet.

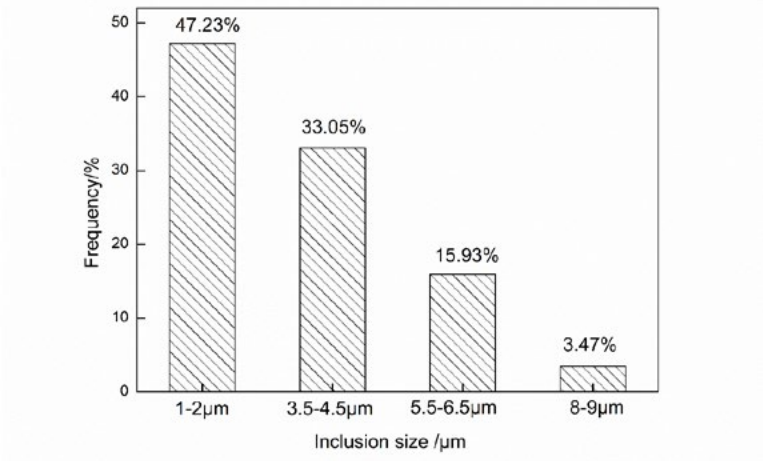

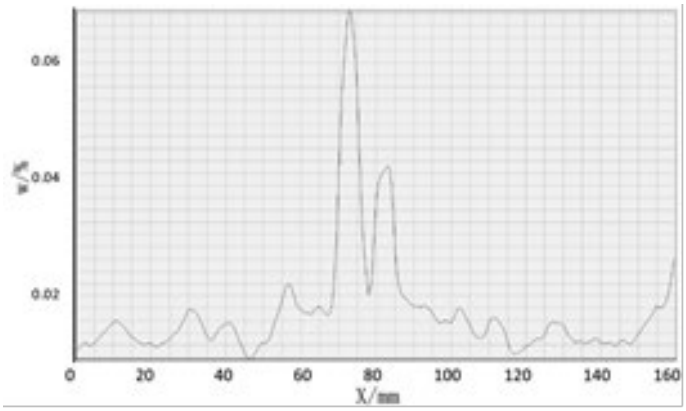

Fig.10 - Content-frequency distribution of Al

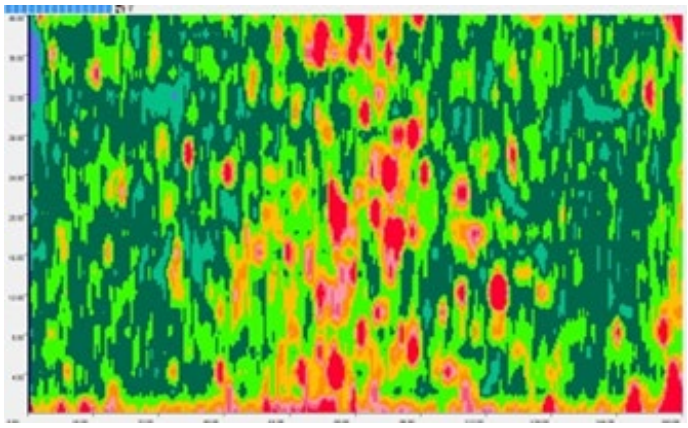

Fig.11 - Two-dimensional distribution of Al

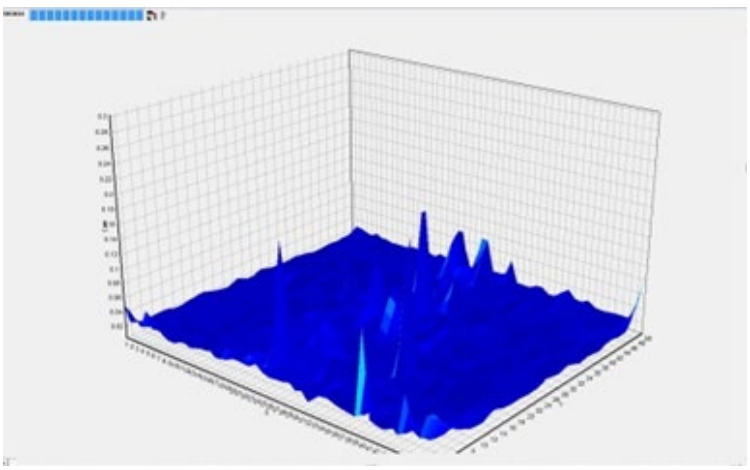

Fig.12 - Three-dimensional distribution of Al

The inclusion in 12Mn steel round billets destroys the uniform structure of metal, especially the large inclusion with diameter greater than 50 μm. In order to obtain non-metal inclusions with the size of greater than 50 μm, the inclusions in 12Mn steel round billet are extracted and separated by Slime method. The inclusions' three –dimensional morphologies are seen in Figure 13, from above results, the numbers of larger inclusions are not significant. Moreover, the experimental results show that the total average inclusions weight is 7.76 mg/10 kg for 4 samples (Table 2), which is a common value. This is due to the fact that the refining time is sufficient (containing LF and VD process), the large inclusions are fully floating up to the surface of molten steel, resulting in fewer large inclusions in 12Mn steel.

Tab.2 - Analysis results of large oxide inclusions in 12Mn steel

Sample	Original weight	Remaining weight	Electrolysis weight	Total inclusions weight		Inclusions' size level			
						<80 μm	80~140 μm	140~300 μm	>300 μm
	kg	kg	kg	mg	mg/10kg	mg	mg	mg	mg
1	4.075	0.989	3.086	1.70	5.51	0.10	0.50	0.70	0.40
2	4.045	0.763	3.282	3.20	9.75	0.60	1.20	1.10	0.30
3	4.154	0.866	3.288	3.40	10.34	1.10	1.50	0.80	-
4	4.113	0.800	3.313	1.80	5.43	0.10	0.80	0.90	-

Note: - represents there is no detected inclusion corresponding to size.

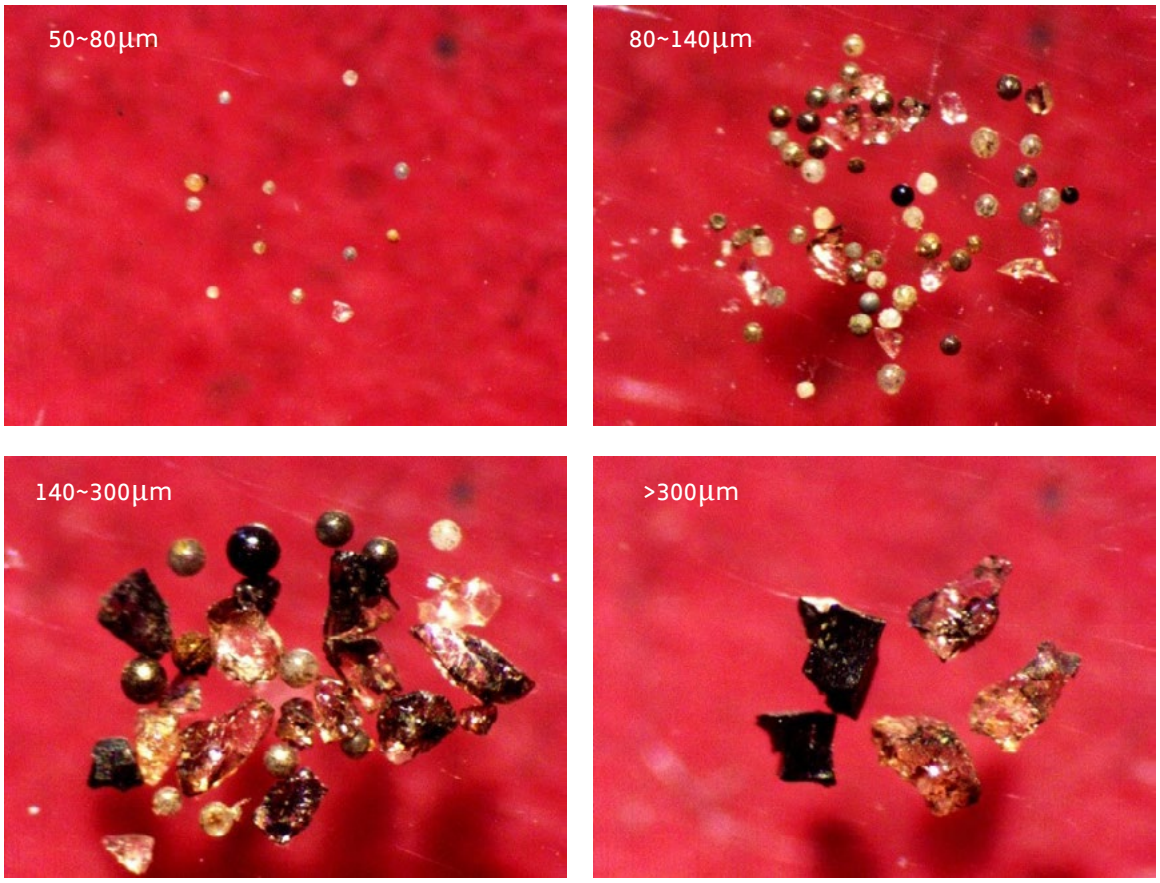

Fig.13 - Large inclusions at 20 magnification

As shown in Figure 14, the ternary diagram of oxides obtained is depending on the chemical composition of MgO, Al_2O_3 and CaO. Every dot in the ternary diagram means the chemical composition of one inclusion. Solid inclusions could lead to clogging of 12Mn steel by attaching to the nozzle during solidification. Inclusions must be in the liquid state to avoid nozzle clogging. But the composition distribution means that the majority of inclusions were solid at casting temperature. There were only several inclusions in the liquid state, as shown by the shaded area (temperature < 1500 °C) in the ternary diagram. The samples obtained from both steady state (S1) and ladle (S2) indicate that most inclusions were near the Al_2O_3 region. Exceeding MgO (greater than 30 pct) could have a result of higher (over 2573 K (2300 °C)) melting point of inclusions, and thus throughout the casting process these inclusions were solid. As plenty of the inclusions were of high melting compositions, so the submerged entry nozzle was dramatically clogged during continuous casting (Figure 15), leading to premature termination of production.

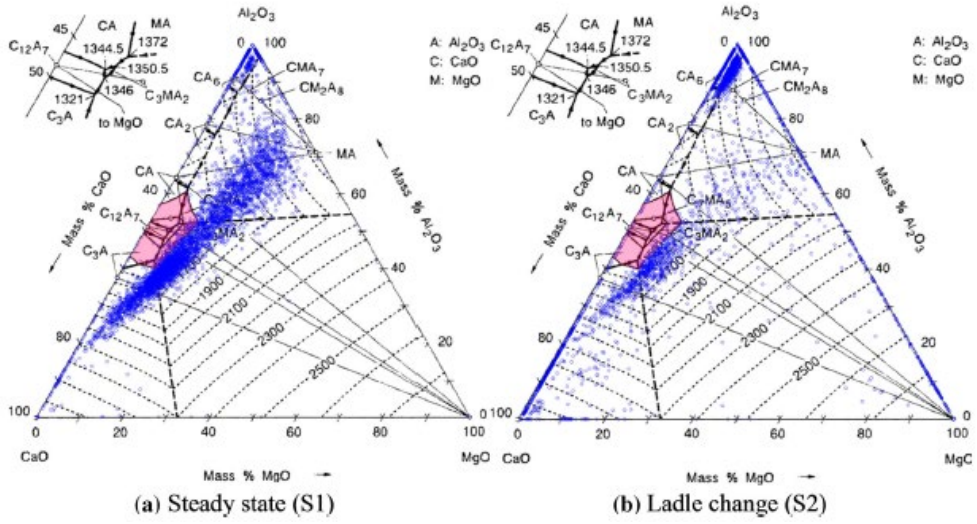

Fig.14 - Al_2O_3-CaO-MgO inclusions in 12Mn steel [34].

Fig.15 - Erosion in the submerged entry nozzle .

As shown in Fig 16, the computed diagram of Al-Ca-O system in 12Mn steel round billet at 2146 K (1873 °C) demonstrates the stable areas of different inclusions formed by [Al], [Ca], and [O]. The interaction activity coefficient and the logK for the formation in 12Mn molten steel were different from others. [30–34] Thus, the activity of oxide products is deemed to be unity. The numerical value of the dotted circles represents the oxygen content. The [Al] and [Ca] content in 12Mn steel must be set in the shaded region to prevent nozzle clogging in Figure 16. The Al_2O_3-3CaO and $7Al_2O_3$-12CaO inclusions remain liquid at 2146 K (1873 °C) among all Al-Ca-O inclusions. The [Ca] and [Al] contents in 12Mn steel shown in Table 1 were located in the Al_2O_3-rich area, implying that the calcium treatment was effective and more Ca was required.

The Equilibrium diagram of inclusions during casting of 12Mn steel with composition (Table 1) was computed with the help of the thermodynamic software FactSage using ''FACT53'', ''Ftoxid,'' and ''FSstel'' databases[35] and is illustrated in Figure 17. When [Ca] in 12Mn steel was 2 ppm, MgO•Al_2O_3 spinel inclusions cause the clogging of submerged entry nozzle, due to its high melting point and high hardness. During the period of solidification, liquid inclusions were modified to $CaMg_2Al_{16}O_{27}$ and CaS. After the temperature attained nearly 1573 K(1300 °C), most of MnS and some of TiN secondary phase could precipitate. When [Ca] reaching from 5 to 10 ppm (Figures 17(b) and (c)), most of the spinel inclusions diminished and finally disappeared, as a result, only liquid inclusions remained in the molten steel. MnS inclusions were changed to CaS by coping with calcium treatment. When adding more calcium (Figures 17(d) and (e)), CaS and li-

quid particles were obtained in molten steel, leading to the result of clogging the submerged entry nozzle. Hence, controlling of the composition and refining are beneficial to the last consequence on the casting process.

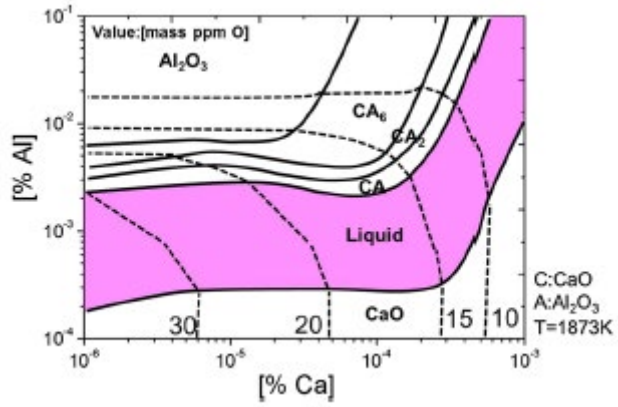

Fig.16 - Calculated stability diagram of Al-Ca-O system in the molten steel at 2146 K (1873°C [34].

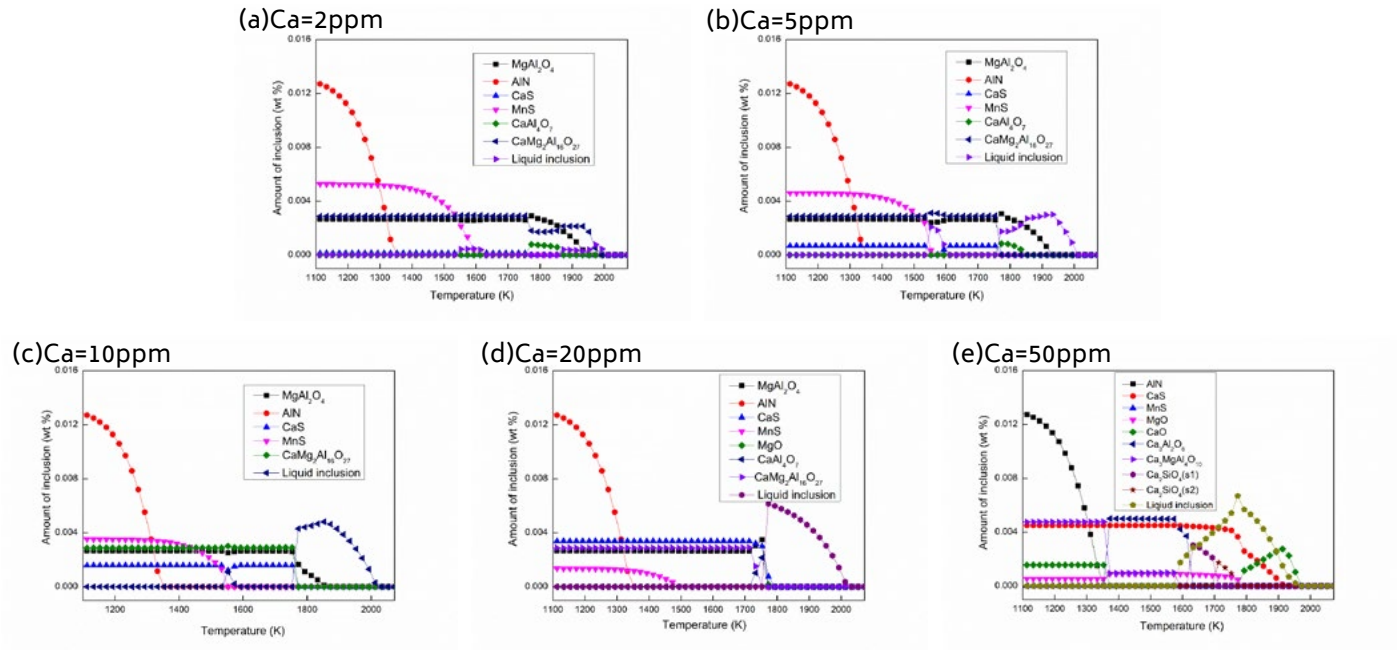

Fig.17 - Equilibrium diagram of inclusions during solidification for 12Mn steel of composition: Fe-0.1C-0.28Si-1.24Mn-0.002S-0.0006Mg-0.0025O-0.0045N-0.03Al-Ca in mass pct.

CONCLUSIONS

Automated particle analysis was widely used to explore inclusions in 12Mn steel continuous casting round billet. The conclusions were summarized:

(1) Automated particle analysis was used to provide an accurate and quick scanning in a certain area to obtain information on inclusions, such as morphology, size, spatial distribution and composition.

(2) The experimental results are in good agreement with the thermodynamic calculation, indicating that most of the inclusions remained solid at casting temperature with few in the liquid as inclusions are not changed by the refining process.

ACKNOWLEDGMENTS

The authors are grateful for financial supporting and experimental help from the Tianjin Iron and Steel Group Co., Ltd., Tianjin, China.

REFERENCES

[1] L. Zhang and B.G. Thomas: ISIJ Int., 2003, vol. 43 (3), pp. 271–91.
[2] T. Ehara, Y. Kurose, and T. Fujimura: 79th Steelmaking Conference Proceeding, ISS, Warrendale, PA, 1996, vol. 79, pp. 485–86.
[3] L. Zhang and B.G. Thomas: 7th European Electric Steelmaking Conference, Venice, Italy, Associazione Italiana di Metallurgia,Milano, 2002, vol. II, pp. 277–86.
[4] L. Zhang, B.G. Thomas, K. Cai, L. Zhu, and J. Cui: ISSTech2003, ISS, Warrendale, PA, 2003, pp. 141–56.
[5] L. Zhang: Steel Res. Int., 2006, vol. 77 (3), pp. 258–69.
[6] L. Zhang: J. Iron. Steel Res. Int., 2006, vol. 13 (4), pp. 1–8.
[7] L. Zhang and B.G. Thomas: Metall. Mater. Trans. B, 2006,vol. 37B, pp. 733–61.
[8] S. Liu, S. Niu, M. Liang, C. Li, X. Zuo, L. Zhang, and X. Wang: Proceedings of AISTech 2007 Iron & Steel Technology Conference and Exposition, AIST, Warrendale, PA, 2007, vol. II, pp. 771–80.
[9] S. Liu, X. Zuo, L. Zhang, S. Niu, M. Liang, C. Li, and X. Wang: Clean Steel 2007, 2007, pp. 272–82.
[10] X. Zuo, M. Long, J. Gao, Y. Wang, and L. Zhang: Iron Steel Technol., 2010, vol. 7 (10), pp. 65–76.
[11] Y. Ren, Y. Chen, X. Yang, S. Yang, L. Zhang, X. Ding, J. Li, S. Li, and F. Liu: AISTech 2012 Proceedings, 2012, pp. 1171–77.
[12] Y. Ren, L. Zhang, S. Yang, and W. Yang: AISTech 2013 Proceedings, 2013, pp. 1159–66.
[13] R. Kiessling: Met. Sci., 1980, vol. 15 (5), pp. 161–72.
[14] R. Rastogi and A.W. Cramb: 2001 Steelmaking Conference Proceedings, ISS, Warrendale, 2001, vol. 84, pp. 789–829.
[15] S. Li, L. Zhang, and X. Zuo: Proceedings of Materials Science and Technology (MS&T) 2008,AIST,Warrendale,PA, 2008, pp. 1259–69.
[16] K. Kawamura, S. Watanabe, and M. Yamada: Tetsu-to-Hagane, 1972, vol. 58 (14), pp. 2060–66.
[17] L. Zhang, S. Li, J. Wang, and X. Zuo: Iron Steel (Chin.), 2009, vol. 44 (3), pp. 75–80.
[18] W. Yang, X. Wang, L. Zhang, and W. Wang: Steel Res. Int., 2013,vol. 84 (9), pp. 878–91.
[19] J. Tan and P.C. Pistorius: AISTech 2013 Iron and Steel Technology Conference, May 6, 2013–May 9, 2013, Pittsburgh, PA, U.S.A.,Association for Iron and Steel Technology, AISTECH, 2013, vol.1, pp. 1301–11.
[20] P.C. Glaws, R.V. Fryan, and D.M. Keener: 74th Steelmaking Conference Proceedings, ISS, Warrendale, PA, 1991, vol. 74, pp. 247–64.
[21] M. Iwasaki, N. Suzuki, T. Ohshiro, H. Utsumi, K. Miyake, and K.Sahara: R&D Res. Dev. Kobe Steel Eng. Rep., 1985, vol. 35 (3),pp. 73–76.
[22] R.C. Sussman, M. Burns, X. Huang, and B.G. Thomas: 10th Process Technology Conference Proceedings, Iron and Steel Society, Warrendale, PA, 1992, vol. 10, pp. 291–304.
[23] C. Bonilla: 78th Steelmaking Conference Proceedings, ISS, Warrendale, PA, 1995, vol. 78, pp. 743–52.
[24] H. Gao: Steelmaking (Chin.), 2000, vol. 16 (2), pp. 38–43.
[25] M. Goransson, F. Reinholdsson, and K. Willman: I Smaker, 1999, vol. 26 (5), pp. 53–58.
[26] Q. Zhang, L. Wang, and X. Wang: ISIJ Int., 2006, vol. 46 (10),pp. 1421–26.
[27] http://www.aspexcorp.com/Solutions/Software/MQAtrade.aspx.
[28] F. Schamber: Introduction to Automated Particle Analysis by Focused Electron Beam, ASPEX Corporation, Report, 2009.
[29] V. Singh, S. Lekakh, and K. Peaslee: 62nd SFSA Technical and Operating Conference, 2008.
[30] The Japan Society for the Promotion of Science: Steelmaking Data Sourcebook, Gordon and Breach Science, New York, 1988.
[31] B. Hallstedl: J. Am. Ceram. Soc., 1990, vol. 73 (1), pp. 15–23.
[32] H. Itoh, M. Hino, and S. Ban-Ya: Metall. Mater. Trans. B, 1997, vol. 28B, pp. 953–56.
[33] H. Ohta and H. Suito: Metall. Mater. Trans. B, 1997, vol. 28B, pp. 1131–39.
[34] Ren Y , Wang Y , Li S , et al. Detection of Non-metallic Inclusions in Steel Continuous Casting Billets[J]. Metallurgical & Materials Transactions B, 2014, 45(4):1291-1303.
[35] http://www.factsage.com/.